Title
Frequency Tunable Attosecond Apparatus

Authors
Mashiko, Hiroki
Bell, M Justine
Beck, Annelise R
et al.

Publication Date
2014

DOI
10.1007/978-3-319-00521-8_4

Peer reviewed

Chapter 4
Frequency Tunable Attosecond Apparatus

Hiroki Mashiko, M. Justine Bell, Annelise R. Beck, Daniel M. Neumark, and Stephen R. Leone

Abstract The development of attosecond technology is one of the most significant recent achievements in the field of ultrafast optics; it opens up new frontiers in atomic and molecular spectroscopy and dynamics. A unique attosecond pump-probe apparatus using a compact Mach-Zehnder interferometer is developed. The interferometer system is compact ($\sim$290 cm^2) and completely located outside of the vacuum chamber. The location reduces the mechanical vibration from vacuum components such as turbopumps and roughing pumps. The stability of the interferometer is $\sim$50 as RMS over 24 hours, stabilized with an active feedback loop. The pump and probe fields can be easily altered to incorporate multiple colors. In the interferometer, double optical gating optics are arranged to generate isolated attosecond pulses with a supercontinuum spectrum. The frequencies of the attosecond pulses can be selected to be in the extreme ultraviolet (XUV) region (25–55 eV, 140 as) or the vacuum ultraviolet (VUV) region (15–24 eV, $\sim$400 as) by metal filters. Furthermore, the near infrared probe field (1.65 eV) can be upconverted to the ultraviolet (3.1 eV). The frequency tunability in the XUV and VUV is critical for selecting excited states of target atoms and molecules.

H. Mashiko (✉) · M.J. Bell · A.R. Beck · D.M. Neumark · S.R. Leone
Ultrafast X-ray Science Laboratory, Chemical Sciences Division, Lawrence Berkeley National Laboratory, CA, Berkeley, 94720, USA
e-mail: mashiko.hiroki@lab.ntt.co.jp

M.J. Bell · A.R. Beck · D.M. Neumark · S.R. Leone
Department of Chemistry, University of California, CA, Berkeley, 94720, USA

S.R. Leone
Department of Physics, University of California, CA, Berkeley, 94720, USA

H. Mashiko
Material Quantum Optical Physics Research Group, Optical Science Laboratory, NTT Basic Research Laboratory, 3-1, Morinosato Wakamiya, Atsugi-shi, Kanagawa 243-0198, Japan

K. Yamanouchi et al. (eds.), *Progress in Ultrafast Intense Laser Science X*,
Springer Series in Chemical Physics 106, DOI 10.1007/978-3-319-00521-8_4,

4.1 Introduction

The generation of attosecond pulses has had a profound impact on the study of dynamics of electrons in atoms [1–5], molecules [6] and solids [7]. Such pulses are produced by high-order harmonic generation (HHG) with intense field femtosecond laser pulses. Attosecond pulses offer high temporal [8] and spatial coherence [9]. Experimental schemes for measuring atomic and molecular dynamics by coupling an attosecond pulse and an optical laser pulse have been devised utilizing the detection of photons, ions, or photoelectrons [1–8]. Experimental systems in previous work each have individual advantages and disadvantages, but each system requires stabilization with attosecond time resolution and has various optical limitations in the extreme ultraviolet (XUV: 30–250 eV) and vacuum ultraviolet (VUV: 6–30 eV) regions [10]. In this review, we introduce several attosecond pump-probe systems from previous work and discuss their characteristics. Then, we discuss a system using a compact and robust Mach-Zehnder (MZ) type interferometer which can produce frequency tunable isolated attosecond pulses (IAP) and optical probe pulses of several colors. The tunability of the attosecond and optical pulses is important to initiate and probe specific chemical dynamics. Thus, the manipulation of the spectral distribution of the attosecond pulse is a key parameter. This system can generate IAP, using double optical gating (DOG) [11] and metal filters, in either the XUV (25–70 eV) or VUV (15–24 eV) frequency ranges. In addition, the IAP are temporally characterized with both 750 nm (1.6 eV) and 400 nm (3.1 eV) probe fields. The increased flexibility will pave the way for future chemical applications.

4.2 Attosecond Apparatus

4.2.1 Collinear Setup

In the past, a number of configurations have been developed to produce IAP or attosecond pulse trains with pump-probe capabilities, as shown in Fig. 4.1. In this figure, the dashed line indicates the boundary of the vacuum system. The systems have individual characteristics and are designed for specific applications based on photoelectron, photoion, and transient absorption methods. To date, the shortest IAP produced, with a duration of 80 as (bandwidth 55–110 eV), was generated using a collinear system as shown in Fig. 4.1(a) [8]. The advantage of this design is pump-probe stability, because the delay between the XUV beam and near-infrared (NIR) beam is produced by only one optic: a combined XUV multilayer coated mirror and Ag coated mirror [8, 12–14]. Furthermore, the delay can be stabilized with an active feedback loop (stability of 46 as over 33 hours) in order to counteract any slow drifts [15]. In addition, the multilayer mirror can be designed to select specific attosecond frequencies. The disadvantage of this system is that the probe pulse at the target is the residual NIR light from the HHG upconversion pulse, which collinearly propagates with the IAP. Thus, it is difficult to install extra optics to control this field.

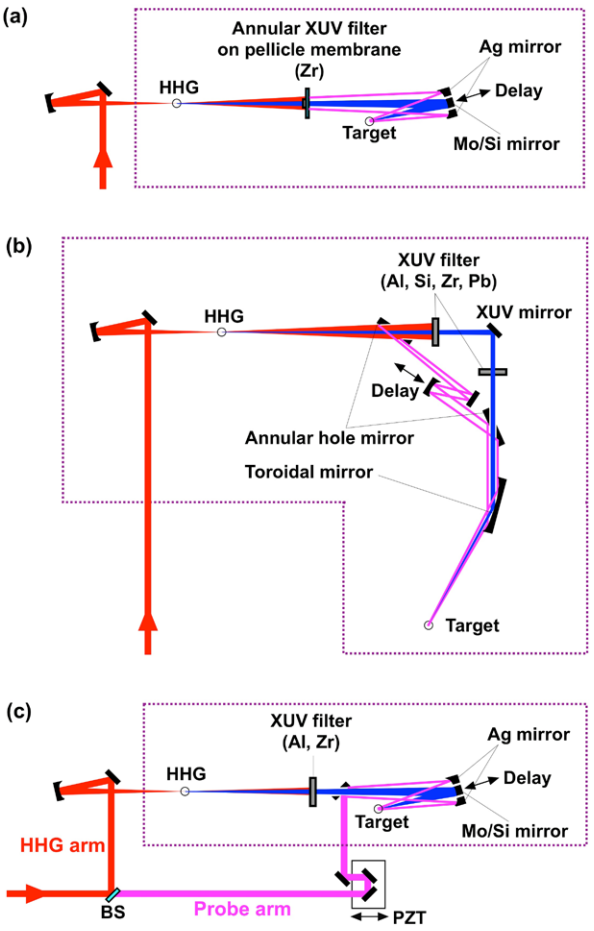

Fig. 4.1 Various configurations to produce attosecond pulses with merging XUV/VUV and NIR fields. FS: Fused silica plate, HHG: high harmonic generation, PZT: piezo-electronic transducer

4.2.2 Large MZ Interferometer Setup

With a MZ interferometer setup, it is easier to control the optical characteristics of the pump and probe pulses. Figure 4.1(b) shows an interferometer located after the high harmonics are generated [16]. The NIR field can be controlled with various optics such as a neutral density filter or a focusing mirror. However, the system is more complex and harder to operate compared to the collinear setup in Fig. 4.1(a). Also, the interferometer has a long propagation distance of several meters. Thus, an active stabilization loop was installed, which achieves 50 as stability over 1 hour with 2.5 ms (400 Hz) integration time (limited by the piezoelectric transducer response time). Although the stability is excellent, the feedback loop cannot compensate for the mechanical vibrations of 1 kHz frequency from vacuum turbopumps.

Fig. 4.1 (*Continued*)

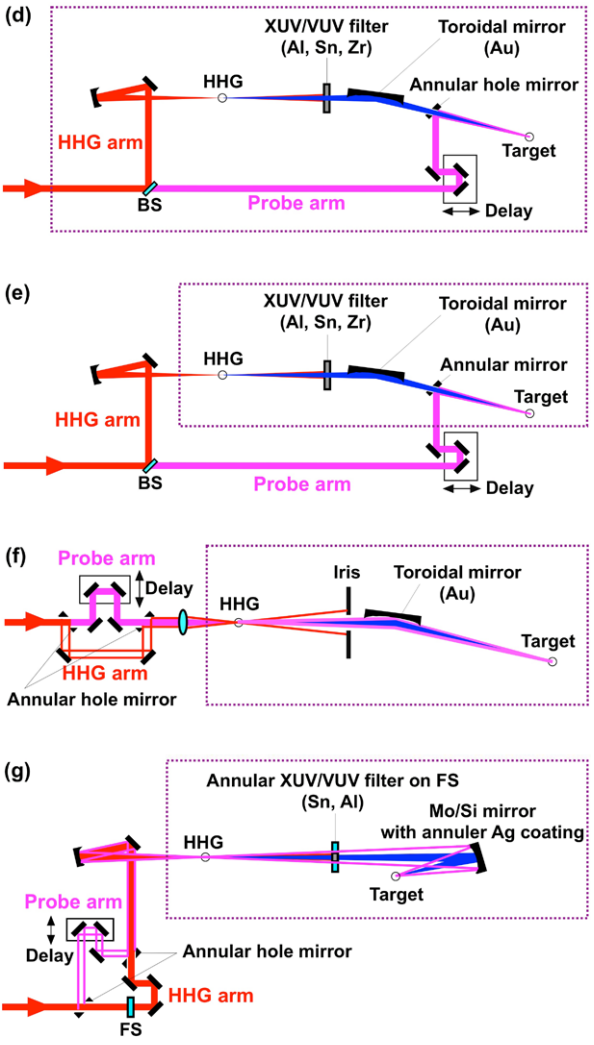

Figure 4.1(c) shows another type of MZ interferometer setup. One arm of the interferometer is located outside the vacuum chamber [17–19]. Thus, it is easy to access this arm to install optics. But, due to the extremely sensitive attosecond experiment, air fluctuations cannot be ignored. Thus, an active feedback loop was installed in the interferometer, which shows a stability of ∼8 as RMS (measured at 20 Hz) [19].

Another key technology is focusing optics for the XUV/VUV beam. In Fig. 4.1(d), the system is equipped with a Au coated toroidal mirror instead of a multilayer coated mirror [20–29]. The toroidal mirror allows broadband reflection and high reflectivity at grazing incidence [30], but it is difficult to machine and polish the mirror to the required surface figure and roughness. In this geometry, it is more

difficult to focus the XUV beam than in the normal incidence case [31–34]. In addition, since many groups combine the XUV beam and the probe beam after HHG, the toroidal mirror configuration requires a longer propagation distance [20–29]. In order to improve the stability, some groups have built a robust interferometer inside the vacuum chamber [20, 28]. In another configuration, one arm is located outside of the chamber with an active feedback loop as shown in Fig. 4.1(e) [29]. Due to the large propagation distance, stabilization of the interferometer is critical and difficult to achieve.

4.2.3 Compact MZ Interferometer Setup

In order to solve the stabilization and complex manipulation issues, a compact MZ type interferometer was developed as shown in Fig. 4.1(f) [35]. The HHG driving laser (outer beam) is combined with the probe laser (inner beam) before the HHG cell. The interferometer is located completely outside of the vacuum chamber. After the HHG cell, the HHG driving beam is blocked by an iris and the probe NIR beam and harmonics collinearly propagate to the target. This arrangement is very stable owing to its compact size and the fact that it can be placed a significant distance from mechanical and turbo pumps. Another advantage is that it is easy to access both arms and to control the fields since the interferometer is outside the vacuum chamber. However, the system has three disadvantages. First, the two NIR pulses are overlapped in time and interfere at the HHG cell. Thus, even if the NIR probe pulse is much weaker than the HHG driving pulse, the generated harmonic spectrum is dramatically changed due to the highly nonlinear process of HHG. This effect is similar to the one encountered in two-color gating [36–43]. Second, since the harmonics and NIR probe beams are spatially overlapped and collinearly propagating, a metal filter cannot be installed. Then, the low order harmonic components (3rd, 5th, 7th, etc.) cannot be blocked. The gate width for the lower order harmonics is wider in time than the width for higher orders, so it is difficult to create the IAP with these low order harmonics, even if polarization gating [44] or DOG [11, 45] is used. Third, the HHG driving laser creates a dense plasma in the HHG cell [46, 47]. Thus, the NIR pulses are temporally stretched and spatially defocused due to the large material dispersion of the plasma [10].

In order to address these difficulties, we have developed a new compact MZ interferometer system as shown in Fig. 4.1(g) [48]. An inner beam (the HHG arm) passes through a fused silica plate (1 mm thick). In another arm, the outer beam (the probe arm) is reflected by an annular hole mirror. The stability of the interferometer with a 30 Hz active feedback loop (limited by CCD camera exposure time) is ~50 as RMS over 24 hours. The fused silica produces a large group delay (~5 ps) to the HHG driving pulse relative to the probe pulse. Thus, the two pulses do not temporally overlap in the HHG cell, nor do they interfere in the HHG process. Also, the fused silica plate in the interferometer produces a group delay dispersion in the pulse from the HHG arm relative to the pulse from the probe arm. As a result, the

probe arm pulse is temporally stretched at the HHG cell; the HHG pulse is compressed while the dispersion in the probe pulse is overcompensated. Therefore, the probe arm pulse has a lower peak intensity ($<1 \times 10^{13}$ W/cm^2) so it cannot generate high harmonics. In addition, the NIR probe pulse passes through the HHG cell ~5 ps earlier than the HHG driving pulse in the HHG cell. Thus, the probe pulse isn't temporarily stretched by a dense plasma created by the HHG driving pulse. The generated harmonic beam passes through a metal filter mounted in the center portion of an annular filter that blocks the co-propagating HHG driver beam and low order harmonic beams (3rd, 5th, 7th, etc.). The probe beam passes through the outer portion of the annular filter, a 1 mm thick fused silica plate. In order to reduce energy loss from diffraction, the filter is constructed so that it is the optical image of the last annular hole mirror in the interferometer. The thickness of the fused silica plate is chosen to match the plate in the HHG arm. Then, the probe pulse is compressed and the XUV and probe pulses are temporally overlapped in the target. A spherical mirror with the center part coated with Mo/Si and the outer ring coated with Ag focuses the beams to the target. As mentioned above, due to the MZ interferometer, the probe field can also be upconverted from 750 nm to 400 nm with an achromatic half-wave plate and a β-BaB_2O_4 (BBO) crystal. Further details of the 400 nm probe pulse generation and experimental conditions are described in Ref. [48]. Thus, with this simple system, it is possible to easily manipulate the power, polarization, and frequency of both pulses independently.

4.3 Frequency Tunable IAP with DOG

As mentioned above, the shortest IAP (80 as) were generated with linearly polarized 3.5 fs driving laser pulses [8]. This generation scheme extends the harmonic cutoff region up to 3.5 keV using 3 mJ, 12 fs pulses [49]. However, IAPs can only be produced near the cutoff region of the harmonics, which in practice is greater than 70 eV [50]. Double optical gating (DOG) [11, 51, 52] and polarization gating [20, 44] with elliptically polarized fields allow the generation of IAP in either the plateau region or the cutoff region of the harmonic spectrum because the HHG driving field is effectively gated to one half-cycle (1.3 fs). In particular, DOG has been used to generate an IAP with a 25–620 eV supercontinuum spectrum, which would support a 16 as pulse duration assuming flat phase [52].

In order to generate IAP in our system, a carrier-envelope (CE) phase stabilized Ti:Sapphire oscillator/chirped pulse amplifier followed by a hollow-core fiber compressor produces 7 fs, 1 mJ pulses centered at 750 nm wavelength with a 1 kHz repetition rate. In this laser system, the CE phase stability is ~150 mrad RMS using a 30 Hz feedback loop. Figure 4.2(a) shows DOG optics. Two quartz plates (250 μm and 480 μm thickness) are inserted in the HHG arm in Fig. 4.1(g), and the BBO crystal (150 μm thickness) is located before the HHG cell inside the vacuum chamber. The BBO crystal can also be used to produce the second harmonic of the probe field. Figure 4.2(b) shows the typical harmonic spectrum (upper figure) with

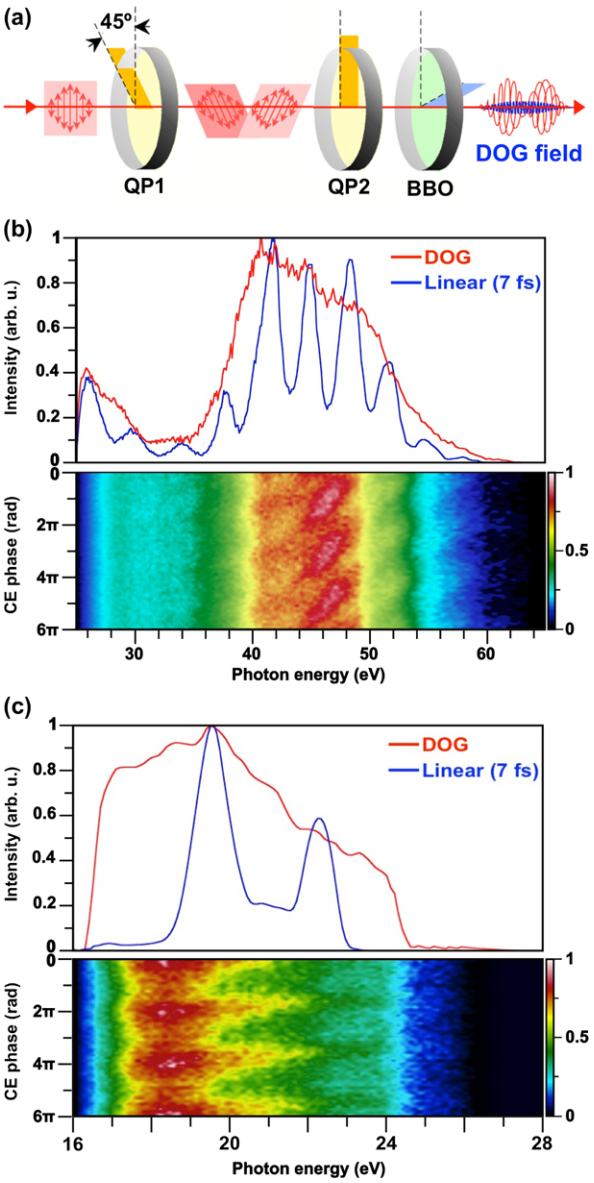

Fig. 4.2 DOG setup (**a**) and typical high-harmonic spectrum with linearly polarized pulse and DOG (*upper figure*) and CE phase dependence with DOG (*lower figure*) using (**b**) an Al filter for the XUV region and (**c**) a Sn filter for the VUV region. QP1: Quartz plate (250 μm), QP2: Quartz plate (480 μm), and BBO: β-BaB_2O_4 (150 μm)

a linearly polarized pulse and with DOG: the lower figure shows the CE phase dependence of the harmonic spectrum with DOG. Both panels were obtained using an Al filter. Analogous results using a Sn filter are shown in Fig. 4.2(c). Demonstrated here, the spectral bandwidth can be filtered by Al and Sn filters.

4.4 Temporal Characterization of IAP in XUV and VUV Regions

In order to characterize the pulses, the attosecond streak camera technique is used [53]. This technique is basically a cross-correlation of the XUV/VUV field and the probe field. Photoelectrons created by the IAP are given a momentum shift by the probe field. The photoelectron kinetic energy distribution is analyzed using a linear photoelectron time-of-flight spectrometer and measured as a function of delay time between the XUV/VUV and probe pulses [48]. The measured streak trace contains information about the temporal structure and the phase of the photoelectron wave packet. Figure 4.3(a) shows a measured streak trace with a 750 nm streak field using an Al filter and Ne as the target gas in the photoelectron spectrometer. The temporal profile and phase are reconstructed by the Principal Component Generalized Projections Algorithm method [54]. The temporal profile indicates a 140 as pulse as shown in Fig. 4.3(b). The satellite pulses are suppressed with less than a 1% contribution at 750 nm half ($\pm$1.25 fs) and full ($\pm$2.5 fs) cycles, indicating a well isolated pulse compared to Ref. [8] in which satellite pulses are measured with an 8 % contribution. In addition, the measured and the reconstructed harmonic spectra agree well as shown in Fig. 4.3(c).

Figure 4.4(a) shows the measured streak trace with a 750 nm field using a Sn filter and Ar as the target. The reconstructed temporal profile and phase indicate a 395 as pulse as shown in Fig. 4.4(b). Again, the pre- and post-pulses are suppressed to less than a 1 % contribution at the 750 nm half and full cycle regions. In addition, the measured and the reconstructed harmonic spectra agree well as shown in Fig. 4.4(c). These results indicate the flexibility of selecting the XUV or VUV frequency range. Of course, in future experiments, if other HHG gases (He, Ne, Kr, Xe, etc.), different filters (Zr, Si, Ti, Pb, etc.) [30], and/or various multilayer coated mirror (SiC/Mg, Sc/Si, Al/C, etc.) are used [55], IAPs with different central frequencies can be generated.

Finally, a streak trace is obtained with a 400 nm streak field using an Al filter and Ne as the target as shown in Fig. 4.5(a). The reconstructed temporal profile and phase indicate a 118 as pulse as shown in Fig. 4.5(b). The measured and the reconstructed spectra agree well as shown in Fig. 4.5(c). This result is important for chemical applications of attosecond pulses. For example, a plasmon resonance in a gold or silver nanoparticle can be excited with a pulse at 400 nm [56]. A streaking measurement can investigate the plasmon dephasing time by observing the enhancement of the photoelectron momentum shift due to the field of the plasmon resonance [5]. Frequency control of the excitation pulse allows nanoparticles of varying structures and plasmon resonance frequencies to be studied. The compact MZ interferometer design allows the probe field to be modified independently of the driving HHG field. In future work, the compact interferometer located outside of the vacuum chamber will easily allow the probe field to be modified using, for example, an optical parametric amplifier [57], an adaptive spatial light modulator [58], or THz oscillator [59].

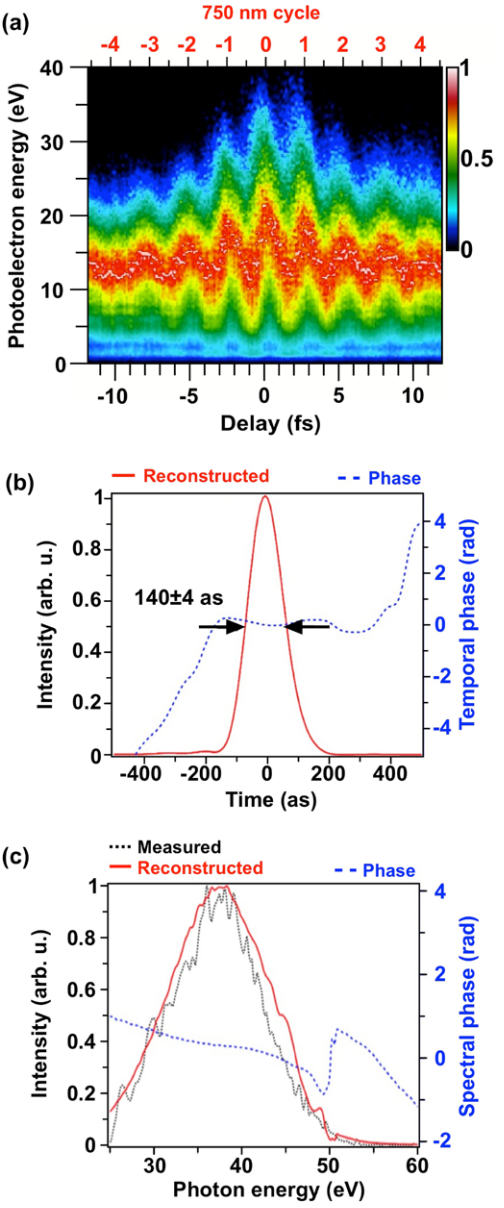

Fig. 4.3 Streak traces and XUV pulse characterization. (**a**) Measured streak trace with Al filter using 750 nm field. (**b**) The reconstructed pulse (*solid line*) and phase (*dotted line*). (**c**) The reconstructed spectrum (*solid line*) and phase (*dotted line*) and the measured spectrum (*dashed line*) without the streak field

4.5 Conclusions

The new setup with compact MZ interferometer realized robust, flexibility, and easy operation. An important step for future attosecond dynamics studies is made by generating IAP with variable center frequencies. XUV and VUV pulses with 140 as duration (26–55 eV) and 395 as duration (16–25 eV), respectively, are characterized.

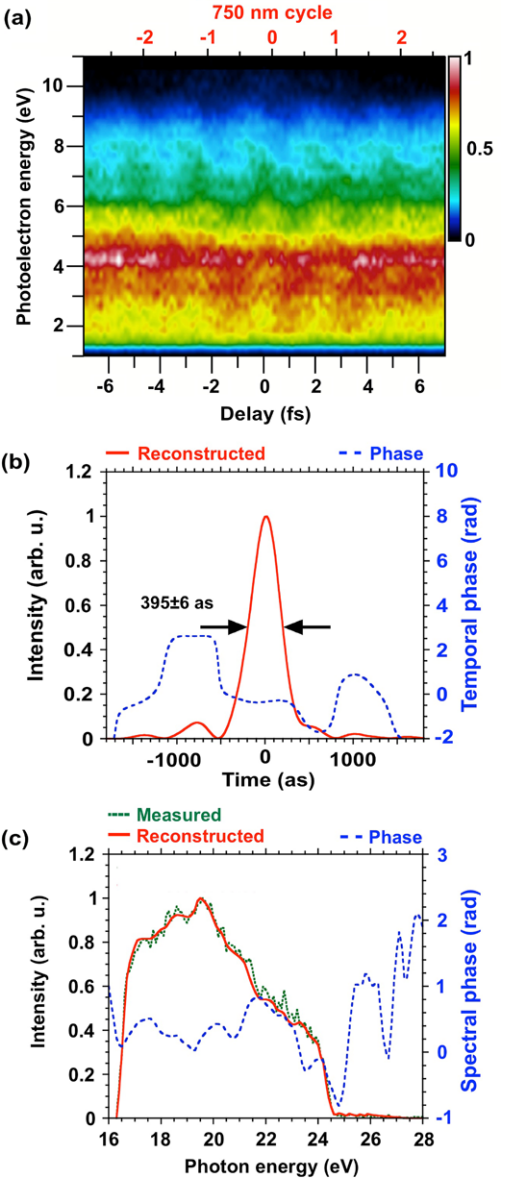

Fig. 4.4 Streak traces and VUV pulse characterization. (**a**) Measured streak trace with Sn filter using 750 nm field. (**b**) The reconstructed pulse (*solid line*) and phase (*dotted line*). (**c**) The reconstructed spectrum (*solid line*) and phase (*dotted line*) and the measured spectrum (*dashed line*) without the streak field

Tunable IAP will allow a greater variety of dynamics in atoms and molecules to be studied. In addition, the characterization of IAP (118 as duration, 26–67 eV) with a streaking measurement using a 400 nm streak field is demonstrated. Many atomic and molecular dynamics processes depend on which states are excited by the light pulses. Frequency control of pump and probe pulses will thus allow the temporal structures and the relative phases of a broader range of ultrafast electronic

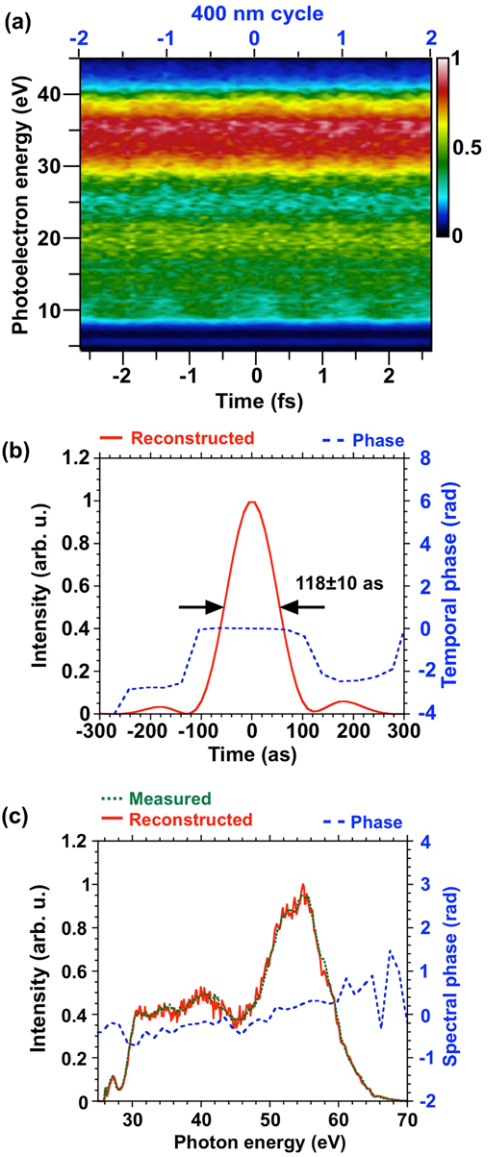

Fig. 4.5 Streak traces and XUV pulse characterization. (**a**) Measured streak trace with Al filter using 400 nm field. (**b**) The reconstructed pulse (*solid line*) and phase (*dotted line*). (**c**) The reconstructed spectrum (*solid line*) and phase (*dotted line*) and the measured spectrum (*dashed line*) without the streak field

and molecular dynamics to be determined. This system and result increased flexibility will allow attosecond experimental techniques to be more widely applied to chemical systems.

Acknowledgements This work was supported by the Director, Office of Science, Office of Basic Energy Sciences, and the Division of Chemical Sciences, Geosciences, and Biosciences, of the U.S. Department of Energy at Lawrence Berkeley National Laboratory under Contract No. DE-AC02-05CH11231. M.J.B. and A.R.B. acknowledge support from National Science Foundation

Graduate Research Fellowships. S.R.L. acknowledges additional support from the National Science Foundation, Chemistry Division, a National Science Foundation, Extreme Ultraviolet Science Engineering Research Center, and a National Security Science and Engineering Faculty Fellowship. The authors thank the LBNL Center for X-Ray Optics (CXRO) for custom made XUV/VUV optics.

References

1. M. Drescher, M. Hentschel, R. Kienberger, M. Uiberacker, V. Yakovlev, A. Scrinzi, Th. Westerwalbesloh, U. Kleineberg, U. Heinzmann, F. Krausz, Time-resolved atomic inner-shell spectroscopy. Nature **419**, 803–807 (2002)
2. R. Kienberger, E. Goulielmakis, M. Uiberacker, A. Baltuška, V. Yakovlev, F. Bammer, A. Scrinzi, Th. Westerwalbesloh, U. Kleineberg, U. Heinzmann, M. Drescher, F. Krausz, Atomic transient recorder. Nature **427**, 817–821 (2004)
3. M. Uiberacker, Th. Uphues, M. Schultze, A.J. Verhoef, V. Yakovlev, M.F. Kling, J. Rauschenberger, N.M. Kabachnik, H. Schröder, M. Lezius, K.L. Kompa, H.G. Muller, M.J.J. Vrakking, S. Hendel, U. Kleineberg, U. Heinzmann, M. Drescher, F. Krausz, Attosecond real-time observation of electron tunnelling in atoms. Nature **446**, 627–632 (2007)
4. E. Goulielmakis, Z.-H. Loh, A. Wirth, R. Santra, N. Rohringer, V.S. Yakovlev, S. Zherebtsov, T. Pfeifer, A.M. Azzeer, M.F. Kling, S.R. Leone, F. Krausz, Real-time observation of valence electron motion. Nature **466**, 739–744 (2010)
5. T. Pfeifer, M.J. Abel, P.M. Nagel, A. Jullien, Z. Loh, M.J. Bell, D.M. Neumark, S.R. Leone, Time-resolved spectroscopy of attosecond quantum dynamics. Chem. Phys. Lett. **463**, 11–24 (2008)
6. G. Sansone, F. Kelkensberg, J.F. Pérez-Torres, F. Morales, M.F. Kling, W. Siu, O. Ghafur, P. Johnsson, M. Swoboda, E. Benedetti, F. Ferrari, F. Lépine, J.L. Sanz-Vicario, S. Zherebtsov, I. Znakovskaya, A. L'Huillier, M.Yu. Ivanov, M. Nisoli, F. Martín, M.J.J. Vrakking, Electron localization following attosecond molecular photoionization. Nature **465**, 763–767 (2010)
7. A.L. Cavalieri, N. Müller, T. Uphues, V.S. Yakovlev, A. Baltuška, B. Horvath, B. Schmidt, L. Blümel, R. Holzwarth, S. Hendel, M. Drescher, U. Kleineberg, P.M. Echenique, R. Kienberger, F. Krausz, U. Heinzmann, Attosecond spectroscopy in condensed matter. Nature **449**, 1029–1032 (2007)
8. E. Goulielmakis, M. Schultze, M. Hofstetter, V.S. Yakovlev, J. Gagnon, M. Uiberacker, A.L. Aquila, E.M. Gullikson, D.T. Attwood, R. Kienberger, F. Krausz, U. Kleineberg, Single-cycle nonlinear optics. Science **320**, 1614–1617 (2008)
9. H. Mashiko, A. Suda, K. Midorikawa, Focusing coherent soft-x-ray radiation to a micrometer spot size with an intensity of 10^{14} W/cm^2. Opt. Lett. **29**, 1927–1929 (2004)
10. D. Attwood, *Soft X-Rays and Extreme Ultraviolet Radiation* (Cambridge University Press, Cambridge, 1999)
11. H. Mashiko, S. Gilbertson, C. Li, S.D. Khan, M.M. Shakya, E. Moon, Z. Chang, Double optical gating of high-order harmonic generation with carrier-envelope phase stabilized lasers. Phys. Rev. Lett. **100**, 103906 (2008)
12. E. Goulielmakis, V.S. Yakovlev, A.L. Cavalieri, M. Uiberacker, V. Pervak, A. Apolonski, R. Kienberger, U. Kleineberg, F. Krausz, Attosecond control and measurement: lightwave electronics. Science **317**, 769–775 (2007)
13. T. Witting, F. Frank, W.A. Okell, C.A. Arrell, J.P. Marangos, J.W.G. Tisch, Sub-4-fs laser pulse characterization by spatially resolved spectral shearing interferometry and attosecond streaking. J. Phys. B, At. Mol. Opt. Phys. **45**, 074014 (2012)
14. I. Thomann, A. Bahabad, X. Liu, R. Trebino, M.M. Murnane, H.C. Kapteyn, Characterizing isolated attosecond pulses from hollow-core waveguides using multi-cycle driving pulses. Opt. Express **17**, 4611–4633 (2009)

15. F.M. Böttcher, B. Manschwetus, H. Rottke, N. Zhavoronkov, Z. Ansari, W. Sandner, Interferometric long-term stabilization of a delay line: a tool for pump–probe photoelectron–photoion-coincidence spectroscopy on the attosecond time scale. Appl. Phys. B, Lasers Opt. **91**, 287–293 (2008)
16. M. Fieß, M. Schultze, E. Goulielmakis, B. Dennhardt, J. Gagnon, M. Hofstetter, R. Kienberger, F. Krausz, Versatile apparatus for attosecond metrology and spectroscopy. Rev. Sci. Instrum. **81**, 093103 (2010)
17. O. Guyétand, M. Gisselbrecht, A. Huetz, P. Agostini, R. Taïeb, A. Maquet, B. Carré, P. Breger, O. Gobert, D. Garzella, J.-F. Hergott, O. Tcherbakoff, H. Merdji, M. Bougeard, H. Rottke, M. Böttcher, Z. Ansari, P. Antoine, Evolution of angular distributions in two-colour, few-photon ionization of helium. J. Phys. B, At. Mol. Opt. Phys. **41**, 051002 (2008)
18. K. Oguri, T. Nishikawa, T. Ozaki, H. Nakano, Sampling measurement of soft-x-ray-pulse shapes by femtosecond sequential ionization of Kr^+ in an intense laser field. Opt. Lett. **29**, 1279–1281 (2004)
19. S. Gilbertson, Y. Wu, S.D. Khan, M. Chini, K. Zhao, X. Feng, Z. Chang, Isolated attosecond pulse generation using multicycle pulses directly from a laser amplifier. Phys. Rev. A **81**, 043810 (2010)
20. G. Sansone, E. Benedetti, F. Calegari, C. Vozzi, L. Avaldi, R. Flammini, L. Poletto, P. Villoresi, C. Altucci, R. Velotta, S. Stagira, S. De Silvestri, M. Nisoli, Isolated single-cycle attosecond pulses. Science **314**, 443–446 (2006)
21. G. Gademann, F. Kelkensberg, W.K. Siu, P. Johnsson, M.B. Gaarde, K.J. Schafer, M.J.J. Vrakking, Attosecond control of electron–ion recollision in high harmonic generation. New J. Phys. **13**, 033002 (2011)
22. E. Mansten, J.M. Dahlström, P. Johnsson, M. Swoboda, A. L'Huillier, J. Mauritsson, Spectral shaping of attosecond pulses using two-colour laser fields. New J. Phys. **10**, 083041 (2008)
23. M. Holler, F. Schapper, L. Gallmann, U. Keller, Attosecond electron wave-packet interference observed by transient absorption. Phys. Rev. Lett. **106**, 123601 (2011)
24. O. Guyétand, M. Gisselbrecht, A. Huetz, P. Agostini, R. Taïeb, A. Maquet, B. Carré, P. Breger, O. Gobert, D. Garzella, J.-F. Hergott, O. Tcherbakoff, H. Merdji, M. Bougeard, H. Rottke, M. Böttcher, Z. Ansari, P. Antoine, Evolution of angular distributions in two-colour, few-photon ionization of helium. J. Phys. B, At. Mol. Opt. Phys. **41**, 051002 (2008)
25. Q. Li, K. Hoogeboom-Pot, D. Nardi, M.M. Murnane, H.C. Kapteyn, M.E. Siemens, E.H. Anderson, O. Hellwig, E. Dobisz, B. Gurney, R. Yang, K.A. Nelson, Generation and control of ultrashort-wavelength two-dimensional surface acoustic waves at nanoscale interfaces. Phys. Rev. B **85**, 195431 (2012)
26. D.H. Ko, K.T. Kim, J. Park, J.-h. Lee, C.H. Nam, Attosecond chirp compensation over broadband high-order harmonics to generate near transform-limited 63 as pulses. New J. Phys. **12**, 063008 (2010)
27. W. Cao, G. Laurent, C. Jin, H. Li, Z. Wang, C.D. Lin, I. Ben-Itzhak, C.L. Cocke, Spectral splitting and quantum path study of high-harmonic generation from a semi-infinite gas cell. J. Phys. B, At. Mol. Opt. Phys. **45**, 074013 (2012)
28. http://www.physics.ohio-state.edu/~dimauro/lab.html
29. M. Chini, H. Mashiko, H. Wang, S. Chen, C. Yun, S. Scott, S. Gilbertson, Z. Chang, Delay control in attosecond pump-probe experiments. Opt. Express **17**, 21459–21464 (2009)
30. B.L. Henke, E.M. Gullikson, J.C. Davis, X-ray interactions: photoabsorption, scattering, transmission, and reflection at E = 50–30000 eV, Z = 1–92. At. Data Nucl. Data Tables **54**, 181–342 (1993)
31. D. Yoshitomi, T. Shimizu, T. Sekikawa, S. Watanabe, Generation and focusing of submilliwatt-average-power 50-nm pulses by the fifth harmonic of a KrF laser. Opt. Lett. **27**, 2170–2172 (2002)
32. C. Valentin, D. Douillet, S. Kazamias, Th. Lefrou, G. Grillon, F. Augé, G. Mullot, Ph. Balcou, P. Mercére, Ph. Zeitoun, Imaging and quality assessment of high-harmonic focal spots. Opt. Lett. **28**, 1049–1051 (2003)

33. E.J. Takahashi, Y. Nabekawa, H. Mashiko, H. Hasegawa, A. Suda, K. Midorikawa, Generation of strong optical field in soft x-ray region by using high-order harmonics. IEEE J. Sel. Top. Quantum Electron. **10**, 1315–1328 (2004)
34. H. Mashiko, A. Suda, K. Midorikawa, Focusing multiple high-order harmonics in the extreme-ultraviolet and soft-x-ray regions by a platinum-coated ellipsoidal mirror. Appl. Opt. **45**, 573–577 (2006)
35. Y. Mairesse, A. de Bohan, L.J. Frasinski, H. Merdji, L.C. Dinu, P. Monchicourt, P. Breger, M. Kovaćev, R. Taïeb, B. Carré, H.G. Muller, P. Agostini, P. Saliéres, Attosecond synchronization of high-harmonic soft x-rays. Science **302**, 1540–1543 (2003)
36. M.D. Perry, J.K. Crane, High-order harmonic emission from mixed fields. Phys. Rev. A **48**, R4051 (1993)
37. H. Eichmann, A. Egbert, S. Nolte, C. Momma, B. Wellege-hausen, W. Becker, S. Long, J.K. McIver, Polarization-dependent high-order two-color mixing. Phys. Rev. A **51**, R3414 (1995)
38. U. Andiel, G.D. Tsakiris, E. Cormier, K. Witte, High-order harmonic amplitude modulation in two-colour phase-controlled frequency mixing. Europhys. Lett. **47**, 42 (1999)
39. T.T. Liu, T. Kanai, T. Sekikawa, S. Watanabe, Significant enhancement of high-order harmonics below 10 nm in a two-color laser field. Phys. Rev. A **73**, 063823 (2006)
40. I.J. Kim, G.H. Lee, S.B. Park, Y.S. Lee, T.K. Kim, C.H. Nam, T. Mocek, K. Jakubczak, Generation of submicrojoule high harmonics using a long gas jet in a two-color laser field. Appl. Phys. Lett. **92**, 021125 (2008)
41. N. Dudovich, O. Smirnova, J. Levesque, Y. Mairesse, M.Yu. Ivanov, D.M. Villeneuve, P.B. Corkum, Measuring and controlling the birth of attosecond XUV pulses. Nat. Phys. **2**, 781–786 (2006)
42. J. Mauritsson, P. Johnsson, E. Gustafsson, A. L'Huillier, K.J. Schafer, M.B. Gaarde, Attosecond pulse trains generated using two color laser fields. Phys. Rev. Lett. **97**, 013001 (2006)
43. Y. Oishi, M. Kaku, A. Suda, F. Kannari, K. Midorikawa, Generation of extreme ultraviolet continuum radiation driven by a sub-10-fs two-color field. Opt. Express **14**, 7230 (2006)
44. I.J. Sola, E. Mével, L. Elouga, E. Constant, V. Strelkov, L. Poletto, P. Villoresi, E. Benedetti, J.-P. Caumes, S. Stagira, C. Vozzi, G. Sansone, M. Nisoli, Controlling attosecond electron dynamics by phase-stabilized polarization gating. Nat. Phys. **2**, 319 (2006)
45. Z. Chang, Controlling attosecond pulse generation with a double optical gating. Phys. Rev. A **76**, 051403R (2007)
46. M.J. Abel, T. Pfeifer, P.M. Nagel, W. Boutu, M.J. Bell, C.P. Steiner, D.M. Neumark, S.R. Leone, Isolated attosecond pulses from ionization gating of high-harmonic emission. Chem. Phys. **366**, 9–14 (2009)
47. A. Jullien, T. Pfeifer, M.J. Abel, P.M. Nagel, M.J. Bell, D.M. Neumark, S.R. Leone, Ionization phase-match gating for wavelength-tunable isolated attosecond pulse generation. Appl. Phys. B **93**, 433–442 (2008)
48. H. Mashiko, M.J. Bell, A.R. Beck, M.J. Abel, P.M. Nagel, C.P. Steiner, J. Robinson, D.M. Neumark, S.R. Leone, Tunable frequency-controlled isolated attosecond pulses characterized by either 750 nm or 400 nm wavelength streak fields. Opt. Express **18**, 25887–25895 (2010)
49. E. Seres, J. Seres, Ch. Spielmann, X-ray absorption spectroscopy in the keV range with laser generated high harmonic radiation. Appl. Phys. Lett. **89**, 181919 (2006)
50. P.B. Corkum, F. Krausz, Attosecond science. Nat. Phys. **3**, 381–387 (2007)
51. X. Feng, S. Gilbertson, H. Mashiko, H. Wang, S.D. Khan, M. Chini, Y. Wu, K. Zhao, Z. Chang, Generation of isolated attosecond pulses with 20 to 28 femtosecond lasers. Phys. Rev. Lett. **103**, 183901 (2009)
52. H. Mashiko, S. Gilbertson, M. Chini, X. Feng, C. Yun, H. Wang, S.D. Khan, S. Chen, Z. Chang, Extreme ultraviolet supercontinua supporting pulse durations of less than one atomic unit of time. Opt. Lett. **34**, 3337–3339 (2009)
53. J. Itatani, F. Quéré, G.L. Yudin, M.Yu. Ivanov, F. Krausz, P.B. Corkum, Attosecond streak camera. Phys. Rev. Lett. **88**, 173903 (2002)
54. D.J. Kane, Principal components generalized projections: a review. J. Opt. Soc. Am. B **25**, A120–A132 (2008)

55. M. Yamamoto, M. Yanagihara, H. Kimura, M. Watanabe, Soft x-ray multilayer optics for use with synchrotron radiation. J. Jpn. Soc. Sync. Rad. Res. **9**, 16–39 (1996) (in Japanese)
56. P.K. Jain, M.A. El-Sayed, Plasmonic coupling in noble metal nanostructures. Chem. Phys. Lett. **487**, 153–164 (2010)
57. A. Shirakawa, I. Sakane, T. Kobayashi, Pulse-front-matched optical parametric amplification for sub-10 fs pulse generation tunable in the visible and near infrared. Opt. Lett. **23**, 1292–1294 (1998)
58. E. Matsubara, K. Yamane, T. Sekikawa, M. Yamashita, Generation of 2.6 fs optical pulses using induced-phase modulation in a gas-filled hollow fiber. J. Opt. Soc. Am. B **24**, 985–989 (2007)
59. K. Tanaka, H. Hirori, M. Nagai, THz nonlinear spectroscopy of solids. IEEE Trans. Terahertz Sci. Technol. **1**, 301–312 (2011)